

# Characterization of the Pentacoordinate Sodium Cations in Hydrated Nucleoside 5'-Phosphates by Solid-State $^{23}\text{Na}$ NMR and Quantum Mechanical Calculations

Alan Wong and Gang Wu\*

Department of Chemistry, Queen's University, Kingston, Ontario, Canada K7L 3N6

Received: August 22, 2002; In Final Form: November 6, 2002

We report a solid-state  $^{23}\text{Na}$  NMR study for the sodium cations in four hydrated disodium salts of nucleoside 5'-phosphates: 2'-deoxycytidine 5'-monophosphate (dCMP), 2'-deoxyguanosine 5'-monophosphate (dGMP), 2'-deoxyuridine 5'-monophosphate (dUMP), and adenosine 5'-triphosphate (ATP). Using one- and two-dimensional solid-state NMR techniques, we were able to detect all crystallographically distinct  $\text{Na}^+$  ions in each of the Na–nucleotide systems. A total of 12 Na sites were fully characterized, among which four exhibit unusual penta-coordination geometry. The present study provides the first reliable solid-state  $^{23}\text{Na}$  NMR characterization for the pentacoordinate  $\text{Na}^+$  ions in nucleoside 5'-phosphates. Spectral assignment was achieved on the basis of quantum mechanical electric-field-gradient (EFG) calculations at the restricted Hartree–Fock level with a 6-31G(d) basis set. The pentacoordinate  $\text{Na}^+$  ion found in  $[\text{d}(\text{TG}_4\text{T})_4]$  by high-resolution X-ray crystallography was modeled by using an isolated guanine quartet together with a central  $\text{Na}^+$  ion and an axial water molecule. Quantum mechanical calculations suggest that the  $^{23}\text{Na}$  quadrupole coupling constant for this square-pyramidal Na site is large (ca. 3 MHz), providing a possible explanation for the previous failure in detecting this type of  $\text{Na}^+$  ions by solid-state  $^{23}\text{Na}$  NMR.

## 1. Introduction

Recent discoveries from X-ray crystallographic, nuclear magnetic resonance (NMR), and molecular dynamics (MD) simulation studies have prompted new discussions regarding the role of alkali metal ions in nucleic acid structures.<sup>1–5</sup> To date, crystallography is the most reliable experimental technique for localizing metal ions in biological structures. However, direct detection of  $\text{Na}^+$  ions in nucleic acids and proteins by crystallography represents a tremendous challenge.<sup>6,7</sup> This is because a  $\text{Na}^+$  ion has the same number of electrons (thus virtually identical X-ray scattering power) as a water molecule, making it difficult to distinguish the two species in electron density maps. In solutions, because the association between  $\text{Na}^+$  ions and biological molecules is weak,  $\text{Na}^+$  ions often undergo rapid exchange between free and bound states. Consequently, solution  $^{23}\text{Na}$  NMR cannot provide *site-specific* information, although the magnetic relaxation dispersion (MRD) method is capable of providing some insightful information about DNA–cation interactions.<sup>8</sup> We recently proposed to use solid-state  $^{23}\text{Na}$  NMR spectroscopy as a complementary approach to X-ray crystallography for detecting  $\text{Na}^+$  ions in biological structures.<sup>9</sup> One important advantage of the solid-state NMR approach is that samples in the forms of powders or lyophilized solids can be directly used in the experiment. Furthermore,  $^{23}\text{Na}$  NMR parameters are a sensitive measure of the local electronic structure at the ion-binding site.<sup>10</sup> In the past two years, solid-state  $^{23}\text{Na}$  NMR studies dealing with molecular systems related to nucleic acids have begun to emerge.<sup>11–14</sup>

In general, a  $\text{Na}^+$  ion prefers to coordinate to six ligand atoms forming an octahedral coordination geometry. However, pentacoordinate  $\text{Na}^+$  ions may also be present in nucleic acid structures. An interesting example of such  $\text{Na}^+$  ions is found

in a G-quadruplex,  $[\text{d}(\text{TG}_4\text{T})_4]$ , where a  $\text{Na}^+$  ion is located within a G-quartet plane coordinating to four keto oxygen atoms and one water molecule.<sup>15</sup> The binding geometry around this  $\text{Na}^+$  ion is a well-defined square pyramid with the water molecule being the axial ligand. Surprisingly, this pentacoordinate Na site was not observed in the solid-state  $^{23}\text{Na}$  NMR spectra of  $[\text{d}(\text{TG}_4\text{T})_4]$ .<sup>11</sup> To our knowledge, pentacoordinate  $\text{Na}^+$  ions have never been ambiguously detected in any Na–nucleotide system by solid-state  $^{23}\text{Na}$  NMR, despite the fact that pentacoordinate  $\text{Na}^+$  ions are quite common in inorganic Na salts.<sup>16</sup> Using a point-charge model, Koller et al.<sup>16</sup> predicted a large quadrupole coupling constant ( $C_Q$ ), ca. 3 MHz, for square-pyramidal Na sites. These results suggest that the pentacoordinate Na site in  $[\text{d}(\text{TG}_4\text{T})_4]$  may have a large  $C_Q$ , which would lead to a broad  $^{23}\text{Na}$  NMR signal. In a recent study, we observed a pentacoordinate Na site in tetrasodium (1,2-ethanediylidinitrilo)tetraacetate pentahydrate,  $\text{Na}_4(\text{EDTA})\cdot 5\text{H}_2\text{O}$ .<sup>17</sup> This pentacoordinate  $\text{Na}^+$  ion is also in a square pyramidal geometry but surprisingly exhibits only an intermediate  $C_Q$  value, 2.06 MHz. One important structural difference between the pentacoordinate  $\text{Na}^+$  ion in EDTA and that in  $[\text{d}(\text{TG}_4\text{T})_4]$  is that, in the former case, the  $\text{Na}^+$  ion is 0.468 Å above the square plane. It may be speculated that such a structural difference is responsible for the very different solid-state  $^{23}\text{Na}$  NMR observations for these two types of pentacoordinate  $\text{Na}^+$  ions. To further understand the relationship between  $^{23}\text{Na}$  NMR parameters and ion-binding geometry, we decided to investigate simple Na salts of nucleoside 5'-phosphates that are known to contain pentacoordinate Na sites on the basis of high-resolution X-ray crystallographic data. In this study, we chose the following mononucleotide systems: disodium 2'-deoxycytidine 5'-monophosphate heptahydrate (dCMP), disodium 2'-deoxyguanosine 5'-monophosphate tetrahydrate (dGMP), disodium 2'-deoxyuridine 5'-monophosphate pentahydrate (dUMP), and disodium adenosine 5'-triphosphate trihydrate (ATP).

\* To whom correspondence should be addressed. Phone: 613-533-2644. Fax: 613-533-6669. E-mail: gangwu@chem.queensu.ca.

In NMR, spectral assignment is always an important problem. It is the first step in any spectral analysis or structural elucidation. In solid-state  $^{23}\text{Na}$  NMR, spectral assignment is particularly difficult, because the relationship between  $^{23}\text{Na}$  NMR parameters (chemical shift and quadrupole parameters) and cation coordination geometry has not been fully understood. Very often, spectral assignment in  $^{23}\text{Na}$  NMR is made on the basis of simple symmetry argument. Although this simple approach may be sufficient in many simple systems, a general approach is definitely needed. In this study, we introduce a combined experimental/theoretical approach to address the spectral assignment problem for  $^{23}\text{Na}$  NMR. The general approach taken in this study consists of two steps. First, we use one- and two-dimensional solid-state  $^{23}\text{Na}$  NMR methods to obtain reliable NMR parameters for all crystallographically distinct Na sites that are present in the crystal lattice. In particular, multiple-quantum magic-angle spinning (MQMAS) NMR<sup>18</sup> is used to achieve spectral separation for different Na sites. Second, we perform quantum mechanical electric-field-gradient (EFG) calculations for appropriately constructed molecular cluster models. By comparing the calculated EFG tensors with the experimental results, a connection can be established between observed  $^{23}\text{Na}$  NMR parameters and individual Na sites. It should be noted that quantum mechanical EFG calculations for  $^{23}\text{Na}$  nuclei have recently been demonstrated to be reliable in both inorganic and organic systems.<sup>19–21</sup> This theoretical approach is used in the present study to aid the spectral assignment for Na–nucleotide systems. Because the chemical shift range for  $^{23}\text{Na}$  nuclei is very small and reliable shielding calculations are difficult, in the present study, we focus only on  $^{23}\text{Na}$  quadrupole parameters for the purpose of spectral assignment.

## 2. Experimental Details

**Materials.** Hydrated disodium salts of 2'-deoxycytidine 5'-monophosphate (dCMP), 2'-deoxyguanosine 5'-monophosphate (dGMP), 2'-deoxyuridine 5'-monophosphate (5'-dUMP), and adenosine 5'-triphosphate (ATP) were obtained from Sigma-Aldrich (Canada). The ATP sample was used without further purification, whereas the dCMP, dGMP, and dUMP samples were carefully crystallized by following the procedures given in the X-ray diffraction studies.<sup>22–24</sup> This recrystallization step is important for these samples because the solid-state  $^{23}\text{Na}$  NMR spectra obtained for materials directly from the bottle were of a much lower quality in spectral resolution than those for freshly recrystallized samples, presumably because of partial dehydration of the samples during storage. We did not observe any significant dehydration after spinning the samples (packed inside a 4-mm rotor) at typically 5–9 kHz for a period of 10–24 h.

**Solid-State NMR.** Solid-state  $^{23}\text{Na}$  NMR spectra were recorded at 11.75 T on a Bruker Avance-500 spectrometer operating at 132.26 and 500.01 MHz for  $^{23}\text{Na}$  and  $^1\text{H}$  nuclei, respectively. The  $^{23}\text{Na}$  chemical shift was referenced to NaCl(aq) by setting the  $^{23}\text{Na}$  NMR signal of a solid NaCl sample to  $\delta = 7.21$  ppm.<sup>25</sup> High-power  $^1\text{H}$  decoupling was applied during all data acquisition. For  $^{23}\text{Na}$  magic-angle spinning (MAS) experiments, the sample spinning frequencies were 8000–8500 with a stability of 2 Hz. Single-pulse excitation with a pulse width of 1.0  $\mu\text{s}$  was used to record one-dimensional MAS spectra. At the same RF power level, the 90° pulse for the central transition was 2.6  $\mu\text{s}$ . Typically, several hundred transients were collected with a recycle delay on the order of 2–5 s. For two-dimensional  $^{23}\text{Na}$  multiple-quantum (MQ) MAS experiments, the sample spinning frequency was  $8500 \pm 2$  Hz. The z-filter

MQMAS pulse sequence<sup>26</sup> was used: P1( $\phi_1$ )–t1–P2( $\phi_2$ )– $\tau$ –P3( $\phi_3$ )–ACQ(t2,  $\phi_4$ ) where  $\phi_1 = (0^\circ)$ ;  $\phi_2 = (0, 0, 60, 60, 120, 120, 180, 180, 240, 240, 300, 300^\circ)$ ;  $\phi_3 = (0, 180^\circ)$ ;  $\phi_4 = (0, 180, 180, 0^\circ)$ , and  $\tau = 20 \mu\text{s}$ . The optimized excitation (P1) and conversion (P2) pulse widths were 5.0 and 2.0  $\mu\text{s}$ , respectively. The pulse width for the selective  $^{23}\text{Na}$  90° pulse (P3) was 18  $\mu\text{s}$ . Typically, 72–360 transients were collected for each of the 128 t<sub>1</sub> increments with a recycle delay of 2–5 s. The hypercomplex data method<sup>27</sup> was used for obtaining pure-phase 2D spectra. The 2D time-domain data were treated with a shear Fourier transformation (FT).

**Quantum Mechanical Calculations.** All quantum mechanical calculations were performed on a SunFire 6800 symmetric multiprocessor system (24 × 900 MHz processors and 24 GB of memory) using the Gaussian98 suite of programs.<sup>28</sup> To reduce the computational time, simplified molecular clusters were used. A general procedure was followed to construct molecular cluster models. First, each cluster model consists of ligands from the first coordination sphere including water molecules and other functional groups such as phosphate, base, and sugar moieties. Second, if a neighboring Na<sup>+</sup> ion is within 4.0 Å from the target Na<sup>+</sup> ion, a point charge of +0.60e (obtained from an Mulliken analysis) is used in the model to replace this neighbor Na<sup>+</sup> ion. Third, experimental X-ray structures are directly used without any geometry optimization.

A special situation occurred regarding the crystal structure of ATP. The original X-ray diffraction data for ATP were reported by Kennard et al. in 1970.<sup>29</sup> Because of the extreme difficulties in growing high-quality ATP single crystals, the very limited diffraction data were obtained from very small crystals and the crystal structure was refined only to  $R = 12.3\%$ . Several years later, Larson<sup>30</sup> used a different refinement method containing bond restraints and obtained a more reasonable structure for ATP. This later structure was used in our ATP model. The positions of the hydrogen atoms were calculated using SHELXTL<sup>31</sup> with standard bond distances: C–H, 0.96 Å; N–H, 0.90 Å; and O–H, 0.85 Å. The total number of atoms in the molecular clusters varies from 26 to 108, depending on the local environment around the target Na<sup>+</sup> ion. The Na/G-quartet structure was optimized at the B3LYP/6–31(d,p) level with a relativistic effective core potential, CRENBL,<sup>32</sup> for the Na atom. The model possesses a  $C_{4h}$  symmetry. The atomic coordinates of this model structure were provided to us by Michael Meyer.<sup>33</sup>

For the Na–nucleotide systems examined in this study, the calculations were performed at the restricted Hartree–Fock (HF) level of theory with a 6-31G(d) basis set. We used both HF/6-31G(d) and B3LYP/6-31G(d) levels of theory in the calculations for the Na/G-quartet model. The principal components of the  $^{23}\text{Na}$  EFG tensor,  $q_{ii}$ , were computed in atomic units (1 au =  $9.717365 \times 10^{21}$  V m<sup>-2</sup>), with  $|q_{zz}| > |q_{yy}| > |q_{xx}|$  and  $q_{zz} + q_{yy} + q_{xx} = 0$ . In solid-state NMR experiments, the measurable quantities are the quadrupole coupling constant ( $C_Q$ ) and the asymmetry parameter ( $\eta_Q$ ). To compare calculated  $^{23}\text{Na}$  EFG results with experimental quadrupole parameters, the following equations were used:

$$C_Q[\text{MHz}] = e^2 q_{zz} Q/h = -243.96 \times Q[\text{barn}] \times q_{zz}[\text{au}] \quad (1)$$

$$\eta_Q = (q_{xx} - q_{yy})/q_{zz} \quad (2)$$

where  $Q$  is the nuclear quadrupole moment of  $^{23}\text{Na}$ ,  $e$  is the elementary charge, and  $h$  is the Planck constant. In this study, we use the standard  $Q$  value for  $^{23}\text{Na}$ , 0.104 barn, as suggested by Pyykkö<sup>34</sup> (1 barn =  $10^{-28}$  m<sup>2</sup>).

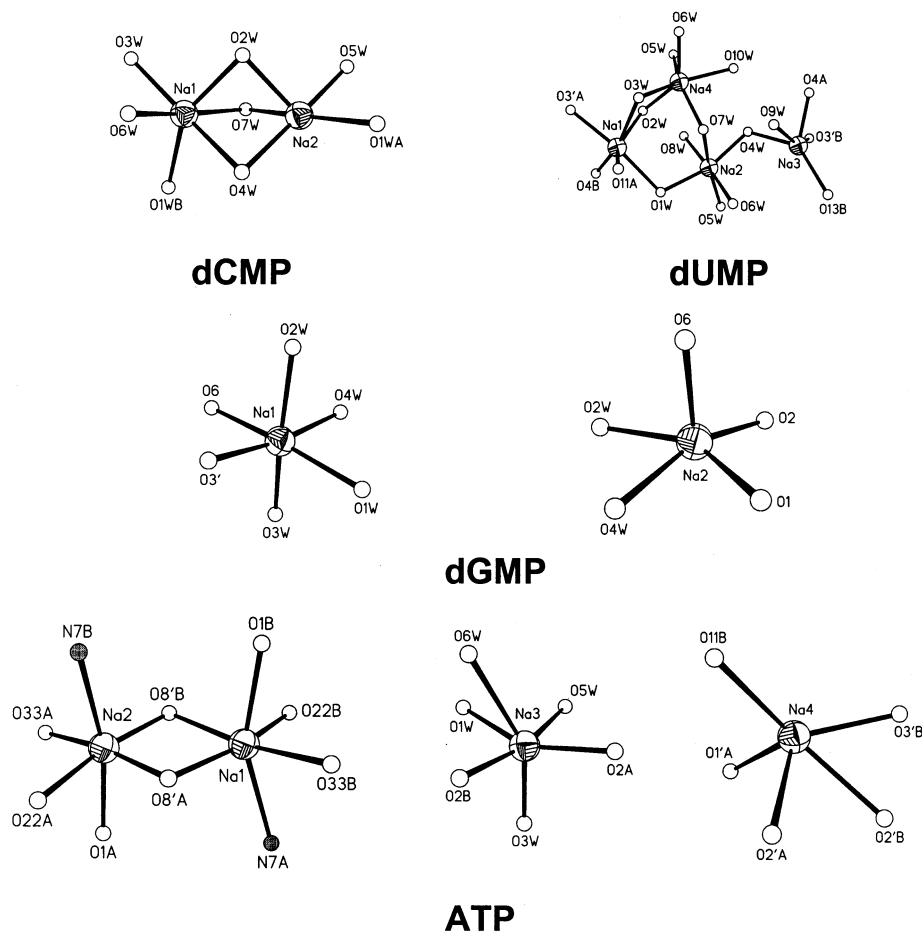


**Figure 1.** Diagram of the Na<sup>+</sup> ion coordination in dCMP, dGMP, dUMP, and ATP.

### 3. Results and Discussion

**Solid-State NMR.** Each of the four Na nucleotides (dCMP, dGMP, dUMP, and ATP) studied in this work contains multiple, crystallographically distinct Na sites in the crystal lattice. Figure 1 shows the ion coordination environment for each of the Na<sup>+</sup> ions in dCMP, dGMP, dUMP, and ATP. On the basis of ion coordination geometry, two types of Na<sup>+</sup> ions are observed in these nucleotide systems: penta- or hexacoordinate Na<sup>+</sup> ions. The ligands coordinating to the Na<sup>+</sup> ions include water, base, sugar, and phosphate groups. The nucleotides chosen in this study exhibit a variety of Na coordination geometries that are good representatives of Na–nucleotide systems.

Figure 2 shows the 1D <sup>23</sup>Na MAS NMR spectra for the four Na-nucleotide systems. Except for the <sup>23</sup>Na MAS spectrum of dCMP, it is very difficult or nearly impossible to extract accurate site-specific NMR information from the broad (sometimes featureless) line shapes observed in these <sup>23</sup>Na MAS spectra. To analyze these ill-defined NMR line shapes, we applied the 2D MQMAS approach. Figure 3 shows the 2D MQMAS spectra of dGMP, dUMP, and ATP. In contrast to the 1D MAS spectra shown in Figure 2, the 2D MQMAS spectra exhibit well-resolved spectral regions, each corresponding to a crystallographically distinct Na site. Combining the observed peak positions in the isotropic *F*<sub>1</sub> dimension ( $\delta_{\text{iso},3Q}^{\text{obs}}$ ) and the *F*<sub>2</sub> cross-section sub-spectra, we were able to accurately simulate the 1D <sup>23</sup>Na MAS spectra and obtain <sup>23</sup>Na NMR parameters for individual Na sites in dGMP, dUMP, and ATP. The observed and simulated 1D MAS spectra are also shown in Figure 2. The experimental <sup>23</sup>Na NMR parameters for the four Na nucleotides are summarized in Table 1. It is important to point

out that the final <sup>23</sup>Na NMR parameters were obtained by examining both the fit in the 1D MAS spectra and the agreement between the observed ( $\delta_{\text{iso},3Q}^{\text{obs}}$ ) and calculated ( $\delta_{\text{iso},3Q}^{\text{cal}}$ ) values, where  $\delta_{\text{iso},3Q}^{\text{cal}}$  is defined as

$$\delta_{\text{iso},3Q}^{\text{cal}} = \delta_{\text{iso}} - \delta_{\text{offset}} + \frac{1}{68} \left( \frac{C_Q}{\nu_L} \right)^2 \left( 1 + \frac{\eta_Q^2}{3} \right) \times 10^6 \quad (3)$$

where  $\nu_L$  is the Larmor frequency for <sup>23</sup>Na. The observed and calculated 3Q positions are also given in Table 1. A plot of  $\delta_{\text{iso},3Q}^{\text{obs}}$  versus  $\delta_{\text{iso},3Q}^{\text{cal}}$  (not shown) yielded a very good straight line (slope = 0.9815 and *R*<sup>2</sup> = 0.9958). It is clear from a comparison of the spectra shown in Figures 2 and 3 that, without the results from the 2D MQMAS spectra, it would be extremely difficult to analyze the 1D <sup>23</sup>Na MAS spectra for dGMP, dUMP, and ATP.

**Spectral Assignment.** Although we have obtained accurate <sup>23</sup>Na NMR parameters for different Na sites in the previous section, it still remains a rather difficult task to assign the observed <sup>23</sup>Na NMR parameters to the appropriate Na sites without ambiguity. In a recent study, we showed that quantum mechanical <sup>23</sup>Na EFG calculations can be used to aid spectral assignment for Na-EDTA complexes.<sup>17</sup> In particular, we found that EFG calculations at both HF and B3LYP levels with split-valence basis sets of 6-31G(d) and 6-311G(d,p) can yield EFG results that are in good agreement with experimental solid-state <sup>23</sup>Na NMR data. Similar levels of quantum mechanical EFG calculations have also been demonstrated to be reliable by Johnson et al.<sup>20</sup> and by Tossell<sup>21</sup> for Na phosphates and for Na macrocyclic systems, respectively. In this study, we decided to

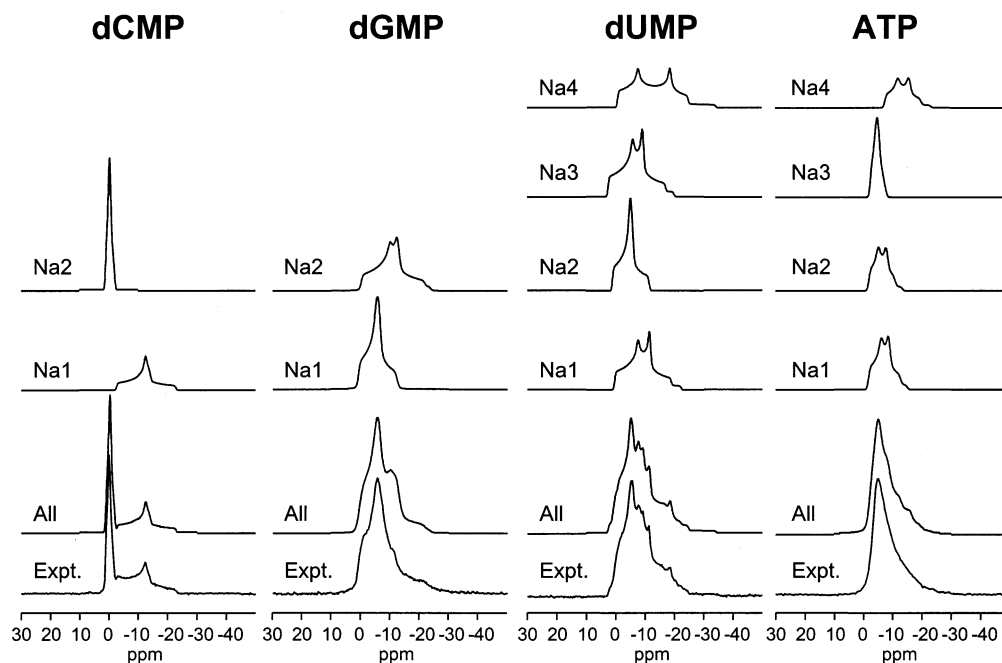


**Figure 2.** Experimental (bottom trace) and simulated (upper trace) 1D  $^{23}\text{Na}$  MAS NMR spectra of dCMP, dGMP, dUMP, and ATP.

use HF/6-31G(d) calculations to assign the  $^{23}\text{Na}$  NMR parameters observed for the four Na–nucleotide systems. The calculated and experimental  $^{23}\text{Na}$  EFG tensor components are reported in Table 2. Figure 4 shows the correlation between the calculated and experimental EFG tensor components (slope = 0.9878 and  $R^2 = 0.9589$ ). The estimated accuracy for the calculated EFG tensor components is approximately 0.5 MHz. Within this accuracy, the Na sites in the four Na–nucleotide systems can be reliably assigned. For example, the two crystallographically distinct Na sites in dCMP have quite different coordination environment.<sup>22</sup> Na1 is hexacoordinate in an octahedral geometry, and Na2 is penta-coordinate in a square pyramidal geometry. Such a difference in Na coordination environment is clearly reflected in the  $^{23}\text{Na}$  MAS spectrum of dCMP, where two well-separated signals are observed; see Figure 1. As seen from Table 2, the quantum mechanical  $^{23}\text{Na}$  EFG calculation indicates that the hexacoordinate  $\text{Na}^+$  ion, Na1, is associated with a small  $C_Q$ ,  $-0.826$  MHz, and the penta-coordinate  $\text{Na}^+$  ion, Na2, has a considerably larger  $C_Q$ , 2.312 MHz. By comparing the magnitude of the calculated  $C_Q$  values with the observed ones for dCMP, 0.85 and 2.20 MHz, it is straightforward to make an assignment for the two signals. Of course, the sign of  $C_Q$  cannot be directly measured by solid-state  $^{23}\text{Na}$  NMR. Assignment for the two Na sites in dGMP was also straightforward. It is also seen in Table 2 that somewhat larger discrepancies exist between the experimental and calculated data for dUMP and ATP. This is probably due to the fact that the crystal structures for dUMP ( $R = 8.9\%$ ) and ATP ( $R = 12.3\%$ ) were much less accurate than those for dCMP ( $R = 4.5\%$ ) and dGMP ( $R = 3.7\%$ ). Nevertheless, it is still possible to make an assignment for the observed  $^{23}\text{Na}$  NMR signals for dUMP and ATP.

**Hexacoordinate Na Sites.** Given that spectral assignment is achieved, it is possible to further examine the relationship between  $^{23}\text{Na}$  NMR data and Na coordination environment in these Na–nucleotide systems. To facilitate discussion, we list in Table 3 a summary of the Na–ligand distances in dCMP, dGMP, dUMP, and ATP. For dCMP, the small  $C_Q$  value observed for Na1, 0.85 MHz, is clearly a consequence of the high symmetry at the Na1 site. According to the crystal structure

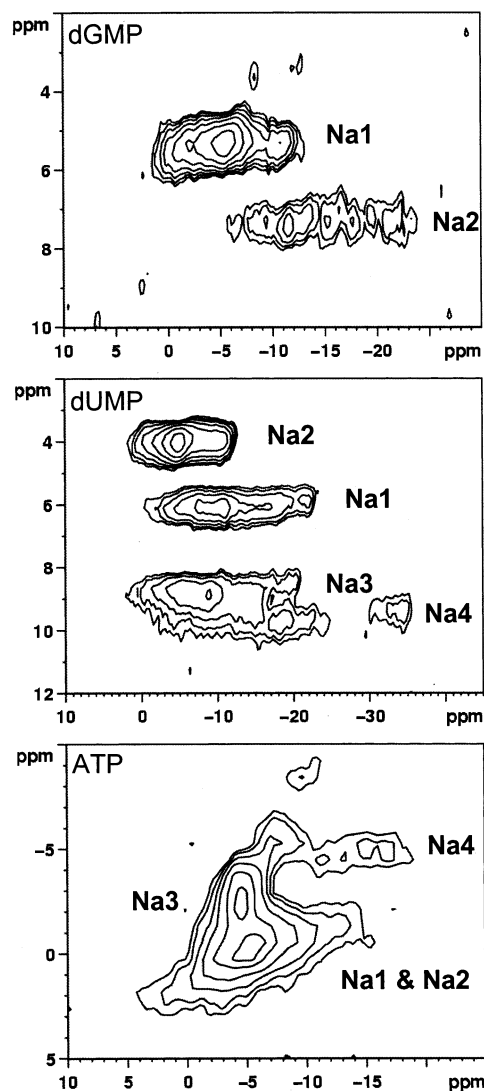


**Figure 3.** Experimental 2D  $^{23}\text{Na}$  MQMAS spectra of dGMP, dUMP, and ATP.

**TABLE 1: Experimental Solid-State  $^{23}\text{Na}$  NMR Parameters for the Na–Nucleotide Systems**

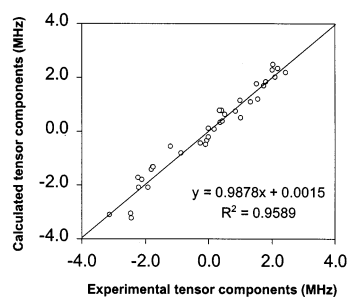
system	site	CN <sup>a</sup>	$\delta_{\text{iso},3Q}^{\text{obs}}/\text{ppm}$ ( $\pm 0.5$ )	$\delta_{\text{iso},3Q}^{\text{cal } b}/\text{ppm}$ ( $\pm 0.5$ )	$C_Q/\text{MHz}$ ( $\pm 0.05$ )	$\eta_Q$ ( $\pm 0.02$ )	$\delta_{\text{iso}}/\text{ppm}$ ( $\pm 0.5$ )
dCMP	Na1	6			0.85	1.00	1.0
	Na2	5			2.20	1.00	-2.6
dGMP	Na1	6	5.3	5.1	1.82	0.90	0.8
	Na2	5	7.2	6.9	2.45	0.80	0.0
dUMP	Na1	6	6.3	6.0	2.45	0.65	0.8
	Na2	6	4.1	3.9	1.75	0.95	1.1
	Na3	5	8.7	8.0	2.42	0.70	2.8
	Na4	6	9.6	9.3	3.12	0.35	1.4
ATP	Na1	6	-0.4	-0.5	1.90	0.60	-1.5
	Na2	6	-0.4	0.0	1.80	0.50	-1.5
	Na3	6	-2.2	-3.0	1.20	0.70	-2.5
	Na4	5	-4.8	-4.9	2.10	0.50	-7.0

<sup>a</sup> Coordination number. <sup>b</sup> The  $\delta_{\text{offset}}$  values for dUMP, ATP, and dGMP are +0.5, +1.9, and -0.7 ppm, respectively.

**TABLE 2: Calculated and Experimental  $^{23}\text{Na}$  EFG Tensor Components<sup>a</sup> for the Na Nucleotide Systems**

system	site	$e^2Qq_{xx}$	$e^2Qq_{yy}$	$e^2Qq_{zz}$	$\eta_Q$
(a) Calculated <sup>b</sup>					
dCMP	Na1	0.087	0.739	-0.826	0.790
	Na2	-0.223	-2.091	2.314	0.807
dGMP	Na1	-0.493	-1.331	1.825	0.459
	Na2	-0.446	-1.737	2.183	0.591
dUMP	Na1	0.767	2.283	-3.050	0.497
	Na2	-0.346	-1.339	1.685	0.589
	Na3	0.775	2.460	-3.235	0.521
	Na4	1.132	1.988	-3.120	0.275
ATP	Na1	0.329	1.761	-2.090	0.685
	Na2	0.359	1.078	-1.437	0.500
	Na3	0.070	0.497	-0.568	0.752
	Na4	0.623	1.180	-1.802	0.309
(b) Experimental <sup>c</sup>					
dCMP	Na1	0.00	0.85	-0.85	1.00
	Na2	0.00	-2.20	2.20	1.00
dGMP	Na1	-0.09	-1.73	1.82	0.90
	Na2	-0.25	-2.21	2.45	0.80
dUMP	Na1	0.43	2.02	-2.45	0.65
	Na2	-0.04	-1.75	1.75	0.95
	Na3	0.36	2.06	-2.42	0.70
	Na4	1.01	2.11	-3.12	0.35
ATP	Na1	0.38	1.52	-1.90	0.60
	Na2	0.45	1.35	-1.80	0.50
	Na3	0.18	1.02	-1.20	0.70
	Na4	0.53	1.56	-2.10	0.50

<sup>a</sup> All EFG components are expressed in MHz (see eq 1). <sup>b</sup> All calculated results were obtained at the HF/6-31(d) level of theory. <sup>c</sup> The signs of the EFG tensor components were assumed on the basis of calculations.

**Figure 4.** Correlation between the observed and calculated  $^{23}\text{Na}$  EFG tensor components for dCMP, dGMP, dUMP, and ATP.

of dCMP,<sup>22</sup> Na1 is coordinated to six water oxygen atoms in an octahedral fashion with a small Na–O<sub>W</sub> distance variation, 2.374–2.579 Å. We noticed that the coordination environment at Na1 of dCMP is very similar to the MP2/6-311G(d,p) fully optimized geometry of a  $[\text{Na}(\text{H}_2\text{O})_6]^+$  cluster,<sup>17</sup> which has an  $O_h$  symmetry with a Na–O<sub>W</sub> distance of 2.432 Å. In fact, Na1

**TABLE 3: Summary of Sodium–Ligand Distances in dCMP, dGMP, dUMP, and ATP**

system	Na–ligand	distance		
		(Å)	(Å)	
dCMP	Na1–O1WB	2.579		
	–O2W	2.406		
	–O3W	2.392		
	–O4W	2.560		
	–O6W	2.374		
	–O7W	2.533		
	Na2–O1WA	2.522		
	–O2W	2.346		
	–O4W	2.423		
	–O5W	2.308		
	–O7W	2.542		
	dUMP	Na1–O1W	2.649	
		–O2W	2.408	
		–O3W	2.891	
–O11A		2.500		
–O3'		2.545		
–O4B		2.257		
Na2–O1W		2.407		
–O4W		2.325		
–O5W		2.376		
–O6W		2.646		
–O7W		2.538		
–O8W		2.576		
Na3–O4W		2.462		
–O9W		2.419		
–O13B	2.436			
–O3'B	2.566			
–O4A	2.274			
Na4–O2W	2.301			
–O3W	2.839			
–O5W	2.950			
–O6W	2.198			
–O7W	2.436			
–O10W	2.513			
dGMP	Na1–O1W	2.527		
	–O2W	2.467		
	–O3W	2.352		
	–O4W	2.381		
	–O3'	2.354		
	–O6	2.559		
	Na2–O2W	2.397		
	–O4W	2.510		
	–O1	2.383		
	–O2	2.322		
	–O6	2.355		
	ATP	Na1–O22B	2.451	
		–O33B	2.667	
		–O8'B	2.473	
–O8'A		2.441		
–O1B		2.581		
–N7A		2.995		
Na2–O22A		2.457		
–O33A		2.515		
–O8'A		2.377		
–O8'B		2.304		
–O1A		2.407		
–N7B		2.636		
Na3–O1W		2.546		
–O3W		2.320		
–O5W	2.642			
–O6W	2.794			
–O2A	2.452			
–O2B	2.446			
Na4–O1'A	2.817			
–O2'A	2.914			
–O2'B	2.932			
–O3'B	2.623			
–O11B	2.665			

of dCMP exhibits the smallest  $C_Q$  among all of the hexacoordinate  $\text{Na}^+$  ions reported in this study. Similar to Na1 of dCMP, Na2 of dUMP is also fully hydrated. For this site, however, the Na–O<sub>W</sub> distances cover a larger range than those around Na1 of dCMP, 2.325–2.646 Å. Consequently, a much larger  $C_Q$  is observed, 1.75 MHz. The hexacoordinate  $\text{Na}^+$  ion in dGMP, Na1, contains two nonwater ligands: one hydroxyl oxygen, O3', and one carbonyl oxygen from the guanine base, O6.<sup>23</sup> Under such a circumstance, although the Na–O distances are still within a small range, 2.352–2.559 Å, which is similar to that found for Na1 in dCMP, the introduction of two nonwater ligands further breaks the electronic symmetry and results in a large increase in  $C_Q$ , 1.82 MHz. This  $C_Q$  is more than twice of that observed for Na1 of dCMP. In the present study, the largest  $C_Q$  observed for  $\text{Na}^+$  ions in an octahedral geometry occurs at

Na1 of dUMP, 2.45 MHz. This large  $C_Q$  is clearly a consequence of the lowest symmetry at this Na site, for which three of the six water molecules are replaced by carbonyl, phosphate and hydroxyl groups at Na–O distances ranging from 2.408 to 2.891 Å.<sup>24</sup>

In addition to geometrical distortion, different types of ligand atoms may further disturb the electronic symmetry at a Na site, resulting in large  $C_Q$  values. For example, each of the Na1 and Na2 sites in ATP is coordinated to five oxygen atoms and one nitrogen atom from the adenine base, whereas Na3 of ATP is coordinated to six oxygen atoms.<sup>29,30</sup> As a result, Na1 and Na2 exhibit somewhat larger  $C_Q$  values, 1.90 and 1.80 MHz, than does Na3, 1.20 MHz, even though all three sites have a similar octahedral geometry. In a previous publication, we reported a similar  $C_Q$  value, 2.30 MHz, for a hexacoordinate Na site with mixed O and N ligands in disodium guanosine 5'-monophosphate heptahydrate.<sup>13</sup>

Unlike other hexacoordinate  $\text{Na}^+$  ions, the coordination geometry at Na4 of dUMP is a distorted trapezoidal bipyramid. In addition, although the six ligands are all water molecules, a large Na– $O_w$  distance variation is present at this Na site, 2.198–2.950 Å. Therefore, a very large  $C_Q$ , 3.12 MHz, is observed for this site. A similar  $C_Q$  was also found for a trapezoidal bipyramidal Na site in  $\text{Na}_4(\text{EDTA})\cdot 5\text{H}_2\text{O}$ , 2.93 MHz.<sup>17</sup> It seems to be a general observation that  $\text{Na}^+$  ions in a trapezoidal bipyramidal geometry have larger  $C_Q$  values than those in an octahedral geometry. This trend is supported by our quantum mechanical calculations and by calculations of Koller et al.<sup>16</sup> on the basis of a point-charge model.

**Pentacoordinate Na Sites.** As mentioned earlier, pentacoordinate  $\text{Na}^+$  ions are of particular interest to us because of their relevance to a unique Na site in  $[\text{d}(\text{TG}_4\text{T})]_4$ . The pentacoordinate  $\text{Na}^+$  ions in dCMP, dGMP, dUMP, and ATP can be divided into three groups. First, the Na2 site of dCMP is fully hydrated. Second, Na2 of dGMP and Na3 of dUMP are partially hydrated. Finally, the Na4 site of ATP is anhydrous. To a crude approximation, these  $\text{Na}^+$  ions all have a distorted square-pyramidal geometry. It is interesting to note that the partially hydrated  $\text{Na}^+$  ions exhibit slightly larger  $C_Q$  values than either the fully hydrated or anhydrous  $\text{Na}^+$  ions. This seems to be in agreement with a simple argument on the basis of electronic symmetry. We also noticed that, in contrast to the observation for hexacoordinate  $\text{Na}^+$  ions, the Na–O distances for the pentacoordinate  $\text{Na}^+$  ions span a relatively small range. Therefore, it appears that the difference in the  $C_Q$  values observed for pentacoordinate  $\text{Na}^+$  ions is due primarily to the nature of the ligand atoms surrounding each Na site and the degree of deviation of the  $\text{Na}^+$  ion from the square plane (vide infra). Furthermore, the partially hydrated pentacoordinate  $\text{Na}^+$  ions in dGMP and dUMP represent innersphere binding sites that are likely to occur in DNAs. For both Na2 of dGMP and Na3 of dUMP, the nonwater ligands are functional groups from the carbonyl, hydroxyl, and phosphate oxygen atoms. As noted earlier, the Na–O distances are also within a narrow range for these partially hydrated  $\text{Na}^+$  ions, i.e., 2.322–2.510 Å for Na2 of dGMP and 2.274–2.566 Å for Na3 of dUMP. However, the  $C_Q$  values for these two Na sites are quite large, 2.45 and 2.42 MHz. In a recent study, we also observed a partially hydrated pentacoordinate  $\text{Na}^+$  ion in  $\text{Na}_4(\text{EDTA})\cdot 5\text{H}_2\text{O}$ , which has a noticeably smaller  $C_Q$  value, 2.06 MHz.<sup>17</sup> The pentacoordinate Na ion in  $\text{Na}_4(\text{EDTA})\cdot 5\text{H}_2\text{O}$  is bound to three acetate oxygen atoms at a Na–O distance range of 2.286–2.344 Å and two water molecules at 2.387 and 2.457 Å. The ion binding environment at this Na site is also square pyramidal. The fact

**TABLE 4: Calculated  $^{23}\text{Na}$  Quadrupole Parameters as a Function of the Na– $O_w$  Distance for the Coplanar  $\text{Na}(\text{H}_2\text{O})\text{G}_4$  Model**

$r(\text{Na}-O_w)/\text{Å}$	HF/6-31G(d)		B3LYP/6-31G(d)	
	$C_Q/\text{MHz}$	$\eta_Q$	$C_Q/\text{MHz}$	$\eta_Q$
2.233	1.899	0.110	1.314	0.238
2.333	2.649	0.057	2.122	0.109
2.371	2.876	0.048	2.379	0.088
2.373	2.885	0.047	2.387	0.087
2.433	3.188	0.036	2.735	0.064
2.533	3.590	0.025	3.208	0.044
2.733	4.146	0.014	3.868	0.025
3.033	4.630	0.009	4.407	0.014
3.233	4.810	0.007	4.574	0.010
3.433	4.913	0.005	4.645	0.008
4.033	5.025	0.003	4.731	0.004
$+\infty^a$	5.135	0.000	4.838	0.000

<sup>a</sup> Calculated without the axial  $\text{H}_2\text{O}$  ligand.

that this Na site exhibits a smaller  $C_Q$  can be attributed to the homology of the three nonwater ligands.

The pentacoordinate site in ATP, Na4, deserves further discussion. For this site, we found the following  $^{23}\text{Na}$  quadrupole parameters:  $C_Q = 2.10$  MHz and  $\eta_Q = 0.50$ . These are in reasonable agreement with the calculated results:  $C_Q = 1.802$  MHz and  $\eta_Q = 0.309$ . This  $\text{Na}^+$  ion is coordinated to three hydroxyl groups, one ether oxygen atom and one phosphate oxygen atom with a small Na–O variation, 2.623–2.932 Å. Recently, Ding and McDowell also reported  $^{23}\text{Na}$  MQMAS NMR spectra for hydrated sodium salt of ATP.<sup>12</sup> However, they obtained significantly different  $^{23}\text{Na}$  quadrupole parameters for the pentacoordinate Na site:  $C_Q = 1.38$  MHz and  $\eta_Q = 0.85$ . In fact, their  $^{23}\text{Na}$  NMR data on other Na sites in ATP are also very different from ours. On examining the published spectra by Ding and McDowell,<sup>12</sup> we noticed that the quality of their NMR spectra was poor, partially because the spectra were obtained at low magnetic fields, 4.7 and 9.4 T. In comparison, the 2D  $^{23}\text{Na}$  MQMAS spectrum shown in Figure 3 for ATP, obtained at 11.75 T, is of much better quality. On the basis of our experimental data and quantum mechanical calculations, we believe that the NMR data shown in Table 1 for ATP are more reliable than those reported by Ding and McDowell.<sup>12</sup>

**Modeling the Pentacoordinate Na Site in  $[\text{d}(\text{TG}_4\text{T})]_4$ .** As mentioned earlier, our search for pentacoordinate  $\text{Na}^+$  ions with a square-pyramidal geometry was motivated by the fact that this type of Na site was observed in  $\text{Na}-[\text{d}(\text{TG}_4\text{T})]_4$  by X-ray crystallography<sup>15</sup> but not by solid-state  $^{23}\text{Na}$  NMR.<sup>11</sup> According to the high-resolution crystal structure of  $[\text{d}(\text{TG}_4\text{T})]_4$ , a  $\text{Na}^+$  ion is essentially coplanar with a G-quartet plane coordinating to four carbonyl oxygen atoms from the guanine bases and a water molecule.<sup>15</sup> The water molecule is located along the  $C_4$  axis of the G-quartet. The distances between the  $\text{Na}^+$  ion and the carbonyl oxygen atoms and the axial water molecule are 2.34 and 2.43 Å, respectively. To estimate the magnitude of  $C_Q$  for this type of Na site, we constructed two G-quartet models, referred to as the coplanar and noncoplanar  $\text{Na}(\text{H}_2\text{O})\text{G}_4$  models in this study. In the coplanar model, a  $\text{Na}^+$  ion is fixed in the G-quartet plane allowing the position of the water molecule to be systematically varied. In the nonplanar model, however, the  $\text{Na}^+$  ion is allowed to deviate from the G-quartet plane. The calculated  $^{23}\text{Na}$  quadrupole parameters for the two G-quartet models are summarized in Tables 4 and 5 and the results are depicted in Figure 5.

It is seen from Table 4 that the magnitude of  $C_Q$  increases monotonically with the distance between the  $\text{Na}^+$  ion and the axial water molecule. If the water molecule is not included in

**TABLE 5: Calculated  $^{23}\text{Na}$  Quadrupole Parameters for the Noncoplanar  $\text{Na}(\text{H}_2\text{O})\text{G}_4$  Model**

$r(\text{Na-G}_4)/\text{\AA}$	HF/6-31G(d)		B3LYP/6-31G(d)	
	$C_Q/\text{MHz}$	$\eta_Q$	$C_Q/\text{MHz}$	$\eta_Q$
(a) $\text{Na-O}_w = 2.320 \text{ \AA}$				
0.000	2.719	0.051	2.219	0.096
0.029	2.702	0.052	2.199	0.099
0.129	2.577	0.060	2.066	0.115
0.229	2.353	0.071	1.844	0.139
0.329	2.047	0.087	1.545	0.176
0.429	1.676	0.114	1.185	0.242
0.529	1.261	0.159	0.783	0.383
0.629	0.823	0.255	0.358	0.868
0.729	0.378	0.579	0.196	0.264
0.829	0.143	0.154	0.495	0.663
(b) $\text{Na-O}_w = 2.820 \text{ \AA}$				
0.000	4.370	0.010	4.140	0.017
0.129	4.271	0.011	4.026	0.019
0.229	4.078	0.012	3.833	0.020
0.329	3.798	0.013	3.560	0.023
0.429	3.450	0.015	3.224	0.026
0.529	3.054	0.018	2.842	0.031
0.629	2.631	0.022	2.432	0.038
0.729	2.198	0.027	2.010	0.048
0.829	1.767	0.035	1.590	0.061

<sup>a</sup>  $r(\text{Na-G}_4)$  is the distance between the  $\text{Na}^+$  ion and the G-quartet plane.

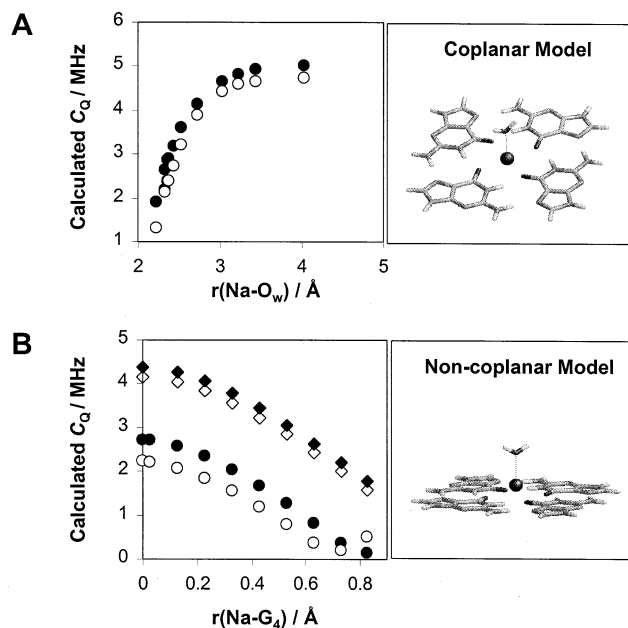


**Figure 5.** (A) Plot of  $C_Q$  as a function of the distance between the  $\text{Na}^+$  ion and the water molecule for the coplanar  $\text{Na}(\text{H}_2\text{O})\text{G}_4$  model. (B) Plot of  $C_Q$  as a function of the distance between the  $\text{Na}^+$  ion and the G-quartet plane for the noncoplanar  $\text{Na}(\text{H}_2\text{O})\text{G}_4$  model. The two models are also shown. Filled symbols: HF/6-31G(d). Open symbols: B3LYP/6-31G(d).

the model, the  $\text{Na}^+$  ion is then in a square-planar geometry. The calculated value of  $C_Q$  for such a Na site is 5.135 MHz. This value is consistent with the prediction of Koller et al. using a point-charge model.<sup>16</sup> We also performed a partial B3LYP/6-31G(d) optimization to determine the most stable position for the water molecule in the coplanar model. The partially optimized structure suggests that the water molecule is 2.371 Å away from the central  $\text{Na}^+$  ion. At this  $\text{Na-O}_w$  distance, the values of  $C_Q$  are 2.876 and 2.379 MHz at the HF/6-31G(d) and B3LYP/6-31(d) level, respectively. Because the  $\text{Na-O}_w$  distance for the pentacoordinate  $\text{Na}^+$  ion in  $[\text{d}(\text{TG}_4\text{T})_4]$  is 2.43 Å, it is expected that the value of  $C_Q$  is approximately 3.0 MHz,

according to the data shown in Figure 5A. This is probably the reason for the previous failure of detecting such pentacoordinate  $\text{Na}^+$  ions in  $[\text{d}(\text{TG}_4\text{T})_4]$  by solid-state  $^{23}\text{Na}$  NMR.<sup>11</sup> It is likely that, in the 1D  $^{23}\text{Na}$  MAS spectra of  $[\text{d}(\text{TG}_4\text{T})_4]$ , the signal from the pentacoordinate  $\text{Na}^+$  ion is obscured by the signals from the phosphate-bound  $\text{Na}^+$  ions. In the 2D MQMAS spectra of  $[\text{d}(\text{TG}_4\text{T})_4]$ , however, the signal from the pentacoordinate  $\text{Na}^+$  ion may be too weak to be observed as a result of a large  $C_Q$ .

For the noncoplanar  $\text{Na}(\text{H}_2\text{O})\text{G}_4$  model, the position of the  $\text{Na}^+$  ion is systematically varied with two constant  $\text{Na-O}_w$  distances, 2.320 and 2.820 Å. Similar to the case for the coplanar model,  $^{23}\text{Na}$  EFG calculations were performed at HF/6-31G(d) and B3LYP/6-31(d) levels. The calculated results are given in Table 5 and displayed in Figure 5B. Figure 5B clearly shows that, as the  $\text{Na}^+$  ion deviates from the G-quartet plane, a decrease in  $C_Q$  is observed. For example, with the  $\text{Na-O}_w$  distance being 2.320 Å, the calculated  $C_Q$  value at the B3LYP/6-31(d) level decreases from 2.22 to 0.50 MHz as the central  $\text{Na}^+$  ion is changed from the in-plane position to being 0.83 Å above the G-quartet plane. This  $C_Q$  dependence provides an explanation for the  $C_Q$  values of 2.0–2.5 MHz observed for the pentacoordinate  $\text{Na}^+$  ions in the Na nucleotides and in  $\text{Na}_4(\text{EDTA})\cdot 5\text{H}_2\text{O}$ , because the pentacoordinate  $\text{Na}^+$  ions in these systems are all slightly noncoplanar.

#### 4. Conclusion

We have presented a combined solid-state  $^{23}\text{Na}$  NMR and quantum mechanical study of four hydrated disodium salts of nucleoside 5'-phosphates. A total of 12 Na sites have been fully characterized. Among these Na sites, two classes of Na coordination are observed: penta- and hexacoordinate  $\text{Na}^+$  ions. The pentacoordinate Na sites are found to have narrowly distributed but larger  $C_Q$  values than the hexacoordinate Na sites. A notable exception is the hexacoordinate  $\text{Na}^+$  ion in trapezoidal bipyramidal geometry, which exhibits the largest  $C_Q$  value among all Na sites. The determination of the  $^{23}\text{Na}$  NMR parameters for pentacoordinate  $\text{Na}^+$  ions bound to nucleotide molecules is the most important finding of the present study. These data represent the first reliable report for this unusual type of  $\text{Na}^+$  ions in nucleotide systems. The  $^{23}\text{Na}$  NMR parameters reported here for mononucleotide systems can serve as benchmarks for future solid-state  $^{23}\text{Na}$  NMR studies of nucleic acids. To date there has been very little solid-state  $^{23}\text{Na}$  NMR data available in the literature for this important class of biological systems. We anticipate that continuing accumulation of solid-state  $^{23}\text{Na}$  NMR data for Na-nucleotide systems will lead to a better understanding of the relationship between  $^{23}\text{Na}$  NMR parameters and Na ion binding structure. The present study has also demonstrated that quantum mechanical EFG calculations at both HF/6-31G(d) and B3LYP/6-31G(d) levels are accurate enough to be useful as a tool for  $^{23}\text{Na}$  NMR spectral assignment. In this study, the  $^{23}\text{Na}$  chemical shift data have not been used for spectral assignment, because the experimental chemical shifts are in a rather small range (ca. 10 ppm). However, as ultrahigh magnetic fields become available, the  $^{23}\text{Na}$  chemical shift will play an increasingly important role in solid-state  $^{23}\text{Na}$  NMR spectroscopy. Meanwhile, it is also expected that reliable magnetic shielding computation for  $^{23}\text{Na}$  nuclei in macromolecular systems will be possible soon. We hope that the present study will provide incentives for future research along these directions.

**Acknowledgment.** G.W. thanks NSERC of Canada for research and equipment grants, Queen's University for a

Chancellor's Research Award, and the Province of Ontario for a Premier's Research Excellence Award. A.W. thanks Queen's University for an R. S. McLaughlin Fellowship and the Province of Ontario for an Ontario Graduate Scholarship (OGS). All quantum mechanical calculations were performed at the High Performance Computing Virtual Laboratory (HPCVL) at Queen's University. We thank Dr. Michael Meyer (Konrad-Zuse-Zentrum Informationstechnik Berlin) for providing the atomic coordinates for an optimized Na/G-quartet structure.

## References and Notes

- (1) Shui, X. Q.; McFail-Isom, L.; Hu, G. G.; Williams, L. D. *Biochemistry* **1998**, *37*, 8341.
- (2) Tereshko, V.; Minasov, G.; Egli, M. *J. Am. Chem. Soc.* **1999**, *121*, 3590.
- (3) Hud, N. V.; Feigon, J. *J. Am. Chem. Soc.* **1997**, *119*, 5756.
- (4) Hud, N. V.; Sklenár, V.; Feigon, J. *J. Mol. Biol.* **1999**, *286*, 651.
- (5) Young, M. A.; Jayaram, B.; Beveridge, D. L. *J. Am. Chem. Soc.* **1997**, *119*, 59.
- (6) Nayal, M.; DiCera, E. *J. Mol. Biol.* **1996**, *256*, 228.
- (7) Tereshko, V.; Wilds, C. J.; Minasov, G.; Prakash, T. P.; Maier, M. A.; Howard, A.; Wawrzak, Z.; Manoharan, M.; Egli, M. *Nucl. Acids Res.* **2001**, *29*, 1208.
- (8) Denisov, V. P.; Halle, B. *Proc. Natl. Acad. Sci. U.S.A.* **2000**, *97*, 629.
- (9) Wu, G. *Biochem. Cell Biol.* **1998**, *76*, 429.
- (10) Wong, A.; Wu, G. *J. Phys. Chem. A* **2000**, *104*, 11844.
- (11) Rovnyak, D.; Baldus, M.; Wu, G.; Hud, N. V.; Feigon, J.; Griffin, R. G. *J. Am. Chem. Soc.* **2000**, *122*, 11423.
- (12) Ding, S.; McDowell, C. A. *Chem. Phys. Lett.* **2000**, *320*, 316.
- (13) Wu, G.; Wong, A. *Chem. Commun.* **2001**, 2658.
- (14) Wong, A.; Fettingner, J. C.; Forman, S. L.; Davis, J. T.; Wu, G. *J. Am. Chem. Soc.* **2002**, *124*, 742.
- (15) (a) Laughlan, G.; Murchie, A. I. H.; Norman, D. G.; Moore, M. H.; Moody, P. C. E.; Lilley, D. M. J.; Luisi, B. *Science (Washington, D.C.)* **1994**, *265*, 520. (b) Phillips, K.; Dauter, Z.; Murchie, A. I. H.; Lilley, D. M. J.; Luisi, B. *J. Mol. Biol.* **1997**, *273*, 171.
- (16) Koller, H.; Engelhardt, G.; Kentgens, A. P. M.; Sauer, J. *J. Phys. Chem.* **1994**, *98*, 1544.
- (17) Wong, A.; Wu, G. *Can. J. Anal. Sci. Spectrosc.* **2001**, *46*, 188.
- (18) Frydman, L.; Harwood, J. S. *J. Am. Chem. Soc.* **1995**, *117*, 5367.
- (19) Tossell, J. A. *Phys. Chem. Minerals* **1999**, *27*, 70.
- (20) Johnson, C.; Moore, E. A.; Mortimer, M. *Chem. Commun.* **2000**, 791.
- (21) Tossell, J. A. *J. Phys. Chem. B* **2001**, *105*, 11060.
- (22) Pandit, J.; Seshadri, T. P.; Viswamitra, M. A. *Acta Crystallogr.* **1983**, *C39*, 342.
- (23) (a) Young, D. W.; Tollin, P.; Wilson, H. R. *Nature (London)* **1974**, *248*, 513. (b) Young, D. W.; Tollin, P.; Wilson, H. R. *Acta Crystallogr.* **1974**, *B30*, 2012. (c) Viswamitra, M. A.; Seshadri, T. P. *Nature (London)* **1974**, *252*, 176.
- (24) Viswamitra, M. A.; Seshadri, T. P.; Post, M. L. *Acta Crystallogr.* **1980**, *B36*, 2019.
- (25) Hayashi, S.; Hayamizu, K. *Bull. Chem. Soc. Jpn.* **1990**, *63*, 913.
- (26) Amoureux, J.-P.; Fernandez, C.; Steuernagel, S. *J. Magn. Reson. Ser. A* **1996**, *123*, 116.
- (27) States, D. J.; Haberkorn, R. A.; Ruben, D. J. *J. Magn. Reson.* **1982**, *48*, 286.
- (28) Frisch, M. J.; Trucks, G. W.; Schlegel, H. B.; Scuseria, G. E.; Robb, M. A.; Cheeseman, J. R.; Zakrzewski, V. G.; Montgomery, J. A., Jr.; Stratmann, R. E.; Burant, J. C.; Dapprich, S.; Millam, J. M.; Daniels, A. D.; Kudin, K. N.; Strain, M. C.; Farkas, O.; Tomasi, J.; Barone, V.; Cossi, M.; Cammi, R.; Mennucci, B.; Pomelli, C.; Adamo, C.; Clifford, S.; Ochterski, J.; Petersson, G. A.; Ayala, P. Y.; Cui, Q.; Morokuma, K.; Malick, D. K.; Rabuck, A. D.; Raghavachari, K.; Foresman, J. B.; Cioslowski, J.; Ortiz, J. V.; Stefanov, B. B.; Liu, G.; Liashenko, A.; Piskorz, P.; Komaromi, I.; Gomperts, R.; Martin, R. L.; Fox, D. J.; Keith, T.; Al-Laham, M. A.; Peng, C. Y.; Nanayakkara, A.; Gonzalez, C.; Challacombe, M.; Gill, P. M. W.; Johnson, B. G.; Chen, W.; Wong, M. W.; Andres, J. L.; Head-Gordon, M.; Replogle, E. S.; Pople, J. A. *Gaussian 98*, revision A.6; Gaussian, Inc.: Pittsburgh, PA, 1998.
- (29) (a) Kennard, O.; Isaacs, N. W.; Coppola, J. C.; Kirby, A. J.; Warren, S.; Motherwell, W. D. S.; Watson, D. G.; Wampler, D. L.; Chenery, D. H.; Larson, A. C.; Ann Kerr, K.; Riva di Sanseverino, L. *Nature (London)* **1970**, *225*, 333. (b) Kennard, O.; Isaacs, N. W.; Motherwell, W. D. S.; Coppola, J. C.; Wampler, D. L.; Larson, A. C.; Watson, D. G. *Proc. R. Soc. London A* **1971**, *325*, 401.
- (30) Larson, A. C. *Acta Crystallogr.* **1978**, *B34*, 3601.
- (31) SHELXTL Crystal Structure Analysis Package, version 5.1; Bruker AXS, Analytical X-ray System; Siemens: Madison, WI, 1998.
- (32) Pacios, L. F.; Christiansen, P. A. *J. Chem. Phys.* **1985**, *82*, 2664.
- (33) Meyer, M.; Steinke, T.; Brandi, M.; Sühnel, J. *J. Comput. Chem.* **2001**, *22*, 109.
- (34) Pyykkö, P. *Mol. Phys.* **2001**, *99*, 1617.